Structural and Multidisciplinary Optimization manuscript No.
(will be inserted by the editor)

Non-uniqueness and Symmetry of Optimal Topology of a Shell for Minimum Compliance

R. Watada · M. Ohsaki · Y. Kanno

Received: date / Revised version: date

Abstract Uniqueness and symmetry of solution are investigated for topology optimization of a symmetric continuum structure subjected to symmetrically distributed loads. The structure is discretized into finite elements, and the compliance is minimized under constraint on the structural volume. The design variables are the densities of materials of elements, and intermediate densities are penalized to prevent convergence to a gray solution. A path of solution satisfying conditions for local optimality is traced using the continuation method with respect to the penalization parameter. It is shown that the rate form of the solution path can be formulated from the optimality conditions, and the uniqueness and bifurcation of the path are related to eigenvalues and eigenvectors of the Jacobian of the governing equations. This way, local uniqueness and symmetry breaking process of the solution are rigorously investigated through the bifurcation of a solution path.

Keywords Topology Optimization · Uniqueness · Symmetry · Shell · Continuation

R. Watada
Dept. of Architecture and Architectural Engineering, Kyoto University, (Currently Takenaka Corporation, Japan, E-mail: watada.ryou@takenaka.co.jp)
M. Ohsaki
Dept. of Architecture and Architectural Engineering, Kyoto University, (Currently Dept. of Architecture, Hiroshima University, 1-4-1, Kagamiyama, Higashi-Hiroshima 839-8527, Japan, E-mail: ohsaki@hiroshima-u.ac.jp)
Y. Kanno
Dept. of Mathematical Informatics, University of Tokyo, Tokyo 113-8656, Japan, E-mail: kanno@mist.i.u-tokyo.ac.jp
A part of this paper was presented at the 8th World Congress of Structural and Multidisciplinary Optimization (WCSMO8).

1 Introduction

There have been numerous studies on topology optimization of two-dimensional continua discretized into finite elements. In most of those studies, the compliance, which is equivalent to the external work against the specified static loads, is minimized under constraint on the total structural volume. The topology optimization problem is regarded as a combinatorial optimization problem using 0–1 variables indicating existence/nonexistence of elements, which are relaxed to continuous variables between 0 and 1. However, simple solution of the relaxed problem leads to a so called gray solution, in which the variables may have intermediate values between 0 and 1.

In order to prevent gray solutions, mainly two approaches have been developed for optimization of plates or sheets; namely, homogenization approach (Bendsøe and Kikuchi, 1988; Suzuki and Kikuchi, 1991) and density approach with penalization (Bendsøe, 1989). The former approach has rigorous mathematical background, but is rather difficult to implement. Therefore, the density approach has been recently preferred especially for structures with nonlinear properties. Because simple application of the density approach in conjunction with a nonlinear programming algorithm results in a gray solution, the intermediate density is penalized to have small stiffness using, e.g., the SIMP (*solid isotropic microstructure with penalty* or *solid isotropic material with penalization*) approach (Rozvany *et al.*, 1992; Bendsøe and Sigmund, 2003; Rozvany, 2009), or penalized to have artificially large structural volume (Bruns, 2005).

Another difficulty in the SIMP approach is the existence of checkerboard solution, which is avoided using the penalization in perimeter length (Petersson, 1999b) or in the gradient of the density (Petersson and Sigmund, 1998). A smoothing filter of the density (Bruns, 2005, 2007) can also be used for regularizing the problem. Optimal topology can be controlled by varying the perimeter length or the parameter value of the filter function. Rietz (2007) obtained various topologies for different values of the gradient parameter. Recently, the level set approach has been developed for simultaneous shape-topology optimization of plates and sheets (Allaire *et al.*, 2002, 2004; Wang *et al.*, 2003; Sethian and Wiegmann, 2000; Yamasaki *et al.*, 2010). Yamada *et al.* (2009) utilized the phase field model in conjunction with the level set approach to control the complexity (number of holes) of optimal topology. However, in these approaches, the intrinsic properties of optimal topology cannot be investigated, because the complexity of the solution is artificially controlled through the penalty terms. Therefore, in this paper, we investigate the properties of the optimal solution using the SIMP approach without additional penalty on the perimeter length or the gradient (slope) of density distribution. Note that it is important for optimization of a symmetric structure that the symmetry property of the solution should be investigated before assigning the types and parameter values for regularization.

In the SIMP approach, a large penalization parameter leads to a 0–1 solution; however, an inappropriate parameter value will restrict symmetry properties and result in a convergence to a local optimal solution which is simply denoted by KKT point satisfying the Karush-Kuhn-Tucker (KKT) conditions. Therefore, a KKT point is usually traced gradually increasing the penalization parameter utilizing the so called *continuation method* (Allgower and Georg, 1993) to select an appropriate value of the penalization parameter as well as the parameters for density filter or penalty of gradients.

It has been shown that the process of gradually increasing the penalization parameter converges to an approximate local optimal solution for the original 0–1 problem (Martínez, 2005) and an exact local solution under certain conditions (Rietz, 2001). In the predictor-corrector continuation method using the Euler predictor, the governing equations are differentiated, and the solution path is traced along the path (Mittelmann and Roose, 1990). This process is basically the same as the parametric programming approach (Gal, 1979; Fiacco, 1983) or the homotopy method (Watson and Haftka, 1989) for tracing KKT points corresponding to the various parameter values (Nakamura and Ohsaki, 1988). However, in most of the continuation methods for the plate (sheet) topology optimization problems (Rozvany *et al.*, 1994), the governing equations are not differentiated, and the solutions are found consecutively with increasing value of the penalization parameter. Stolpe and Svanberg (2001) investigated the trajectory of the optimal solution with respect to the penalization parameter for a problem for minimizing the worst value of compliances under multiple loading conditions.

There have been several papers on topology optimization of shells (Belblidia and Bulman, 2002) including the early paper by Maute and Ramm (1997). Moses *et al.* (2003) investigated symmetric optimal topologies of circular plates assigning the symmetry conditions. However, to the authors' knowledge, there has been no investigation on the mechanism of symmetry-braking process of the optimal topology of an axisymmetric shell. If the penalization parameter is small and intermediate density is allowed, the optimal solution of an axisymmetric shell subjected to symmetric loads is highly likely to be axisymmetric. However, if the intermediate density is penalized, then some ribs should be generated to result in a solution with reduced symmetry. Although the solution with intermediate density has no practical meaning, it is important to investigate the symmetry-breaking process of the KKT point in view of bifurcation of solution paths. In the same manner as bifurcation theory (Ikeda and Murota, 2002), the uniqueness of the solution is strongly related to the symmetry of the solution. Uniqueness and stability of a local optimal solution have been studied by many researchers. Jog and Haber (1996) derived the conditions of stability using incremental form of the variational problem. Petersson (1999a) investigated convergence of the solution with respect to the mesh size for simple loading conditions. Kanno *et al.* (2001) investigated symmetry properties of optimal solutions of semidefinite programming using group theoretic approach, and showed that optimal cross-sectional areas of trusses for maximum eigenvalues are symmetric if the geometry is fixed and symmetric. Stolpe (2010) showed that optimal truss with symmetric geometry and loading conditions may not be symmetric if cross-sectional areas are discrete variables. Rozvany (2011) showed that the solution is usually unique and at least one solution must be symmetric for a symmetric problem with continuous variables.

The purpose of this paper is to investigate the symmetry-reduction process of the local optimal solution. A solution path is defined with respect to the penalization parameter, and a bifurcation point is detected as a singular point of the solution path. This process is carried out without using any filter or penalty for the gradient in order to investigate the intrinsic symmetry-reduction process. We first define local nonuniqueness of the KKT point as a bifurcation of the solution path with respect to the penalization parameter. The formulation for numerical continuation with respect to the penalization parameter is rigorously derived by differentiating the KKT conditions and the stiffness (equilibrium) equations. Then, a condition for local uniqueness of the solution is derived as the singularity of the Jacobian of governing equations (Ohsaki, 2006; Ikeda and Murota, 2002; Ohsaki and Ikeda, 2007). In the numerical examples, the symmetry-reduction process of the optimal solution as a function of the penalization parameter is studied in details. It is shown that a ribbed shell with reduced symmetry is generated through a bifurcation process of the solution path.

2 Conditions for bifurcation of solution path and stability of solution of nonlinear equations

Suppose a set of variables is found as a solution of nonlinear equations defined with a parameter. Then a path or a curve of the solution is defined parametrically in the space of the variables and parameter. In this section, a basic methodology of bifurcation analysis of solution path of nonlinear equations is summarized for the completeness of the paper and to clarify the relation between the stability of iterative solution process and the bifurcation (nonuniqueness) of solution path (Golubitsky and Schaegger, 1979).

Consider a problem of finding the solution $\mathbf{x} \in \mathbb{R}^q$ of the nonlinear equations

$$\mathbf{F}(\mathbf{x}, t) = \mathbf{0} \tag{1}$$

where t is the problem parameter, and $\mathbf{F}(\mathbf{x}, t) \in \mathbb{R}^q$ is continuously differentiable with respect to $\mathbf{x}$ and t. Since the solution is defined by (1) for each specified value of t, it is regarded as a function of t, and is denoted by $\tilde{\mathbf{x}}(t)$. Suppose we have a solution $\tilde{\mathbf{x}}(t^0)$ for $t = t^0$. Then the solution for $t = t^0 + \Delta t$ with a specified increment Δt of t can be estimated using the following linear approximation of the governing equations (1):

$$\mathbf{J}\left[\tilde{\mathbf{x}}(t^0 + \Delta t) - \tilde{\mathbf{x}}(t^0)\right] + \frac{\partial \mathbf{F}}{\partial t}\Delta t = \mathbf{0} \tag{2}$$

where $\mathbf{J} \in \mathbb{R}^{q \times q}$ is the Jacobian of $\mathbf{F}$, for which the (i, j)-component J_{ij} is defined as

$$J_{ij} = \frac{\partial F_i}{\partial x_j}, \quad (i, j = 1, \ldots, q) \tag{3}$$

If $\mathbf{J}$ is nonsingular, then the solution path can be uniquely found using an incremental-iterative method for the governing equations (1) in a similar manner as the arc-length method for geometrically nonlinear equilibrium analysis. In contrast, if $\mathbf{J}$ is singular, then bifurcation of the solution path exists and the solution cannot be determined uniquely at the bifurcation point (Ikeda and Murota, 2002; Ohsaki and Ikeda, 2007).

We next consider a process of finding the solution of (1) for a fixed value of t at t^0 from an arbitrary initial solution using Newton iteration. Let $\mathbf{F}^0$ denote the current value of $\mathbf{F}$ in the iterative process. Then the equation for finding the increment $\Delta\mathbf{x}$ of $\mathbf{x}$ for satisfying (1) with linear approximation is written as

$$\mathbf{F}^0 + \mathbf{J}\Delta\mathbf{x} = \mathbf{0} \tag{4}$$

Therefore, if $\mathbf{J}$ is singular, then the solution of (1) cannot be determined uniquely using (4). Furthermore, if $\mathbf{F}$ is the governing equation of a reciprocal system that has a potential function, then $\mathbf{F}$ is defined as the gradient of the potential, and $\mathbf{J}$ is a symmetric matrix. Therefore, for a reciprocal system, the Newton iteration using (4) diverges if $\mathbf{J}$ is singular. Hence, the solution process is unstable at the bifurcation point of the solution path.

Jog and Haber (1996) derived the conditions of stability using an incremental form of the variational problem for a min-max optimization problem. However, our approach for investigation of uniqueness of the optimal solution based on continuation method is applicable to any type of nonlinear programming problem.

3 Optimization problem and optimality conditions

Consider a symmetric plate or shell discretized into finite elements. The number of elements and the number of degrees of freedom are denoted by m and n, respectively. Let d_j denote the density of the jth element, for which the upper and lower bounds are assigned as

$$0 \leq d_j \leq 1, \quad (j = 1, \ldots, m) \tag{5}$$

The design variable vector is given as $\mathbf{d} = (d_1, \ldots, d_m)^\top$.

Let $\mathbf{P} \in \mathbb{R}^n$ denote the specified nodal load vector. The stiffness matrix is denoted by $\mathbf{K} \in \mathbb{R}^{n \times n}$. Then the nodal displacement vector $\mathbf{U} \in \mathbb{R}^n$ is obtained from the following stiffness (equilibrium) equation:

$$\mathbf{K}(\mathbf{d})\mathbf{U}(\mathbf{d}) = \mathbf{P} \tag{6}$$

The objective function to be minimized is the compliance $W(\mathbf{d})$ defined as

$$W(\mathbf{d}) = \mathbf{P}^\top\mathbf{U}(\mathbf{d}) \tag{7}$$

We use the SIMP approach to prevent gray solutions by penalizing the stiffness of an element with intermediate density. The stiffness matrix $\mathbf{K}$ is defined with the matrix $\mathbf{K}_i \in \mathbb{R}^{n\times n}$ corresponding to the unit density of the ith element and the penalization parameter p as

$$\mathbf{K} = \sum_{i=1}^{m} \{\varepsilon + (1-\varepsilon)d_i^p\}\,\mathbf{K}_i \tag{8}$$

where ε is a sufficiently small positive value for preventing numerical instability. The volume of the ith element is expressed as a product of the area A_i, thickness h_i, and density d_i. Then the problem of minimizing the compliance under a constraint on the total structural volume is formulated with respect to the variable vector $\mathbf{d}$ as

$$\text{minimize} \quad W(\mathbf{d}) = \mathbf{P}^\top \mathbf{U}(\mathbf{d}) \tag{9a}$$

$$\text{subject to} \quad \sum_{i=1}^{m} A_i h_i[\varepsilon + (1-\varepsilon)d_i] - \bar{V} \leq 0 \tag{9b}$$

$$0 \leq d_i \leq 1, \quad (i = 1, \dots, m) \tag{9c}$$

where $\bar{V}$ is the specified upper bound of the total structural volume.

The Lagrangian of Problem (9) is formulated as

$$\begin{aligned} L(\mathbf{d}, \lambda, \boldsymbol{\mu}^{\mathrm{U}}, \boldsymbol{\mu}^{\mathrm{L}}) &= W(\mathbf{d}) \\ &+ \lambda \left(\sum_{i=1}^{m} A_i h_i[\varepsilon + (1-\varepsilon)d_i] - \bar{V} \right) \\ &+ \sum_{i=1}^{m} \mu_i^{\mathrm{U}}(d_i - 1) + \sum_{i=1}^{m} \mu_i^{\mathrm{L}}(-d_i) \end{aligned} \tag{10}$$

where λ, μ_i^{U}, and μ_i^{L} are the Lagrange multipliers that have nonnegative values at the optimal solution. By differentiating (10) with respect to d_i and using (6)–(8), we have

$$\begin{aligned} \frac{\partial L}{\partial d_i} &= -(1-\varepsilon)pd_i^{p-1}\mathbf{U}^\top \mathbf{K}_i \mathbf{U} \\ &\quad + \lambda A_i h_i (1-\varepsilon) + \mu_i^{\mathrm{U}} - \mu_i^{\mathrm{L}} \end{aligned} \tag{11}$$

where the standard approach of sensitivity analysis of compliance has been used (Choi and Kim, 2004). Define $G_i(\mathbf{d})$ as

$$G_i(\mathbf{d}) = -(1-\varepsilon)pd_i^{p-1}\mathbf{U}^\top \mathbf{K}_i \mathbf{U} + \lambda A_i h_i (1-\varepsilon) \tag{12}$$

Then the first-order optimality conditions (KKT conditions) are derived as

$$G_i(\mathbf{d}) \begin{cases} = 0 \text{ for } 0 < d_i < 1 \\ \leq 0 \text{ for } d_i = 1 \\ \geq 0 \text{ for } d_i = 0 \end{cases} \tag{13}$$

The set of indices of elements satisfying $0 < d_i < 1$, and accordingly $G_i(\mathbf{d}) = 0$, is denoted by $\mathcal{I}$; i.e.,

$$\mathcal{I} = \{ i \,|\, 0 < d_i < 1 \} \tag{14}$$

and we define s by $s = |\mathcal{I}|$.

4 Sensitivity of optimal solution with respect to penalization parameter

Equations for computing the sensitivity coefficients with respect to p, which are called parametric sensitivity coefficients for brevity, of the optimal solutions are derived below, where $(\cdot)'$ indicates differentiation with respect to p. For this purpose, the vector of state variables $\mathbf{U}$ and the Lagrange multiplier λ are also regarded as functions of p.

By differentiating (6) with respect to p and using (8), we have

$$\begin{aligned} &-\mathbf{K}\mathbf{U}' - \sum_{i=1}^{m}(1-\varepsilon)pd_i^{p-1}d_i'\mathbf{K}_i\mathbf{U} \\ &\quad = (1-\varepsilon)\sum_{i=1}^{m} d_i^p \ln d_i \mathbf{K}_i \mathbf{U} \end{aligned} \tag{15}$$

By differentiating the volume constraint (9b) and multiplying 1/2, we obtain

$$\frac{1}{2}\sum_{i=1}^{m}(1-\varepsilon)A_i h_i d_i' = 0 \tag{16}$$

Suppose the active side constraints remain active at the KKT point corresponding to the parameter value in the neighborhood of the current value; i.e., $\mu_i^{\mathrm{U}} > 0$ and $\mu_i^{\mathrm{L}} > 0$ are satisfied for $d_i = 1$ and $d_i = 0$, respectively. Furthermore, transition of an inactive side constraint to be active is not considered, because we increase the parameter discretely and find the solution for each specified value of the parameter. Therefore, we can assume that the solution is generally a regular KKT point. Bifurcation at a degenerate point may be investigated similarly using directional derivative of the solution. However, it is shown in the numerical examples that this simple continuation method is practically effective for obtaining a symmetric optimal topology. Hence, for the elements $i \in \mathcal{I}$, differentiation of $G_i(\mathbf{d}) = 0$ with respect to p leads to

$$\begin{aligned} &-(1-\varepsilon)pd_i^{p-1}\mathbf{U}^\top\mathbf{K}_i\mathbf{U}' \\ &\quad - \frac{1}{2}(1-\varepsilon)p(p-1)d_i^{p-2}d_i'\mathbf{U}^\top\mathbf{K}_i\mathbf{U} \\ &\quad + \frac{1}{2}(1-\varepsilon)A_i h_i \lambda' \\ &= \frac{1}{2}(1-\varepsilon)pd_i^{p-1}\ln d_i \mathbf{U}^\top\mathbf{K}_i\mathbf{U} \\ &\quad + \frac{1}{2}(1-\varepsilon)d_i^{p-1}\mathbf{U}^\top\mathbf{K}_i\mathbf{U}, \quad (i \in \mathcal{I}) \end{aligned} \tag{17}$$

For $i \notin \mathcal{I}$, we have $d_i' = 0$. Therefore, there are $n + s + 1$ linear equations (15), (16), and (17) for $n + s + 1$ variables $\mathbf{U}'$, d_i' $(i \in \mathcal{I})$, and λ'.

The indices of elements are rearranged so that $\mathcal{I} = \{1,\dots,s\}$, and define $\mathbf{d}_0 = (d_1,\dots,d_s)^\top$. Then the linear equations for computing the parametric sensitivity coefficients of the KKT point are written in the following form using the notations defined below:

$$\begin{pmatrix} -\mathbf{K} & \mathbf{B}^{12} & \mathbf{0} \\ \mathbf{B}^{12\top} & \mathbf{B}^{22} & \mathbf{B}^{23} \\ \mathbf{0}^\top & \mathbf{B}^{23\top} & 0 \end{pmatrix} \begin{pmatrix} \mathbf{U}' \\ \mathbf{d}_0' \\ \lambda' \end{pmatrix} = \begin{pmatrix} \mathbf{b}^1 \\ \mathbf{b}^2 \\ 0 \end{pmatrix} \tag{18}$$

which is simply written as

$$\mathbf{B}\mathbf{X}' = \mathbf{b} \tag{19}$$

Let $H_i = \mathbf{U}^\top \mathbf{K}_i \mathbf{U}$ and $\mathbf{b}^2 = (b_1^2,\dots,b_s^2)^\top$. The (i,j)-components of $\mathbf{B}^{12} \in \mathbb{R}^{n\times s}$, $\mathbf{B}^{22} \in \mathbb{R}^{s\times s}$, and the ith component of $\mathbf{B}^{23} \in \mathbb{R}^s$ are denoted by B_{ij}^{12}, B_{ij}^{22}, and B_i^{23}, respectively. The jth column of $\mathbf{K}_i$ is denoted by $\mathbf{k}_{ij} \in \mathbb{R}^n$. Then the components of the symmetric matrix $\mathbf{B} \in \mathbb{R}^{(n+s+1)\times(n+s+1)}$ and the constant vector $\mathbf{b} \in \mathbb{R}^{n+s+1}$ are given as

$$B_{ij}^{12} = -(1-\varepsilon)p d_j^{p-1} \mathbf{k}_{ji}^\top \mathbf{U} \tag{20a}$$

$$B_{ii}^{22} = -\frac{1}{2}(1-\varepsilon)p(p-1)d_i^{p-2}H_i, \quad B_{ij}^{22} = 0 \text{ for } i \neq j \tag{20b}$$

$$B_i^{23} = \frac{1}{2}(1-\varepsilon)A_i h_i \tag{20c}$$

$$\mathbf{b}^1 = (1-\varepsilon)\sum_{i=1}^{m} d_i^p \ln d_i \mathbf{K}_i \mathbf{U} \tag{20d}$$

$$b_i^2 = \frac{1}{2}(1-\varepsilon)(1+p\ln d_i)d_i^{p-1}H_i \tag{20e}$$

The path of the optimal solutions can be traced successively solving (19) (Ohsaki and Nakamura, 1996). Since $\mathbf{B}$ is symmetric, the stability of solution is detected from the eigenvalues or the condition number of the matrix.

5 Uniqueness of local optimal solution for specified penalization parameter

We can solve the first equation of (18) for $\mathbf{U}'$ as

$$\mathbf{U}' = -\mathbf{K}^{-1}\mathbf{b}^1 + \mathbf{K}^{-1}\mathbf{B}^{12}\mathbf{d}_0' \tag{21}$$

which is incorporated into the second and third equations of (18) to obtain

$$\begin{pmatrix} \mathbf{B}^{22*} & \mathbf{B}^{23} \\ \mathbf{B}^{23\top} & 0 \end{pmatrix} \begin{pmatrix} \mathbf{d}_0' \\ \lambda' \end{pmatrix} = \begin{pmatrix} \mathbf{b}^{2*} \\ 0 \end{pmatrix} \tag{22}$$

$$\mathbf{b}^{2*} = \mathbf{b}^2 + \mathbf{B}^{12\top}\mathbf{K}^{-1}\mathbf{b}^1, \quad \mathbf{B}^{22*} = \mathbf{B}^{22} + \mathbf{B}^{12\top}\mathbf{K}^{-1}\mathbf{B}^{12} \tag{23}$$

Note that the elements of vector $\mathbf{B}^{23}$ have nonzero values as seen in (20c).

We can see from (20b) that $\mathbf{B}^{22}$ is a diagonal negative definite matrix for $p > 1$, and a null matrix for $p = 1$. In contrast, the matrix $\mathbf{B}^{12\top}\mathbf{K}^{-1}\mathbf{B}^{12}$ is positive definite, because $\mathbf{K}^{-1}$ is positive definite and $\mathbf{B}^{12}$ has full column rank as discussed below. Therefore, the symmetric matrix $\mathbf{B}^{22*}$ is positive definite at $p = 1$, and its lowest eigenvalue may decrease to 0 as p is increased. When $\mathbf{B}^{22*}$ is positive definite, the first equation of (22) can be solved for $\mathbf{d}_0'$ as

$$\mathbf{d}_0' = (\mathbf{B}^{22*})^{-1}(\mathbf{b}^{2*} - \mathbf{B}^{23})\lambda' \tag{24}$$

By incorporating this into the second equation of (22) and using positive definiteness of $(\mathbf{B}^{22*})^{-1}$, we obtain

$$\lambda' = \frac{\mathbf{B}^{23\top}(\mathbf{B}^{22*})^{-1}\mathbf{b}^{2*}}{\mathbf{B}^{23\top}(\mathbf{B}^{22*})^{-1}\mathbf{B}^{23}} \tag{25}$$

Hence, λ' is uniquely determined, and $\mathbf{d}_0'$ is also uniquely found using (24) and (25). Therefore, the parametric sensitivity coefficients of a KKT point are uniquely determined; accordingly, no bifurcation occurs along a solution path if $\mathbf{B}^{22*}$ is nonsingular. This way, the conditions for uniqueness of the solution have been derived using a simple and rigorous manner based on the uniqueness of a solution path.

Note that the matrix $\mathbf{K}$ may be nearly singular and the condition number of $\mathbf{K}^{-1}$ may be very large, if a small value is assigned for ε. However, singularity of $\mathbf{K}$ leads only to nonuniqueness of the displacements that may not have any effect on nonuniqueness of the density variables (Kočvara and Outrata, 2006). In fact, the large eigenvalue of $\mathbf{K}^{-1}$, if exists, corresponds to the eigenmode that has large deformation at the nodes connected by the elements with low density only. Let $\mathbf{f}_i \in \mathbb{R}^n$ denote the vector of equivalent nodal loads of the ith element with $d_i = 1$ corresponding to the displacement vector $\mathbf{U}$. Using (20a), the ith column of $\mathbf{B}^{12}$, denoted by $\mathbf{R}_i \in \mathbb{R}^n$, is given as

$$\mathbf{R}_i = -(1-\varepsilon)p d_i^{p-1}\mathbf{f}_i \tag{26}$$

Hence, $\mathbf{R}_i$ $(i = 1,\dots,s)$ are generally independent, and $\mathbf{B}^{12}$ has full column rank.

The matrix $\mathbf{B}^{12\top}\mathbf{K}^{-1}\mathbf{B}^{12}$ in (23) is denoted by $\mathbf{S} \in \mathbb{R}^{s\times s}$. Then, the (i,j)-component S_{ij} of $\mathbf{S}$ is written as follows using the displacement vector $\mathbf{U}_j \in \mathbb{R}^n$ against $\mathbf{F}_j$:

$$S_{ij} = \mathbf{U}_j^\top \mathbf{R}_i \tag{27}$$

Therefore, the matrix $\mathbf{S} = \mathbf{B}^{12\top}\mathbf{K}^{-1}\mathbf{B}^{12}$ is bounded if the work in the jth element $(j \in \mathcal{I})$ done by the nodal loads that is proportional to the equivalent nodal loads of the ith element $(i \in \mathcal{I})$ is bounded. This condition is

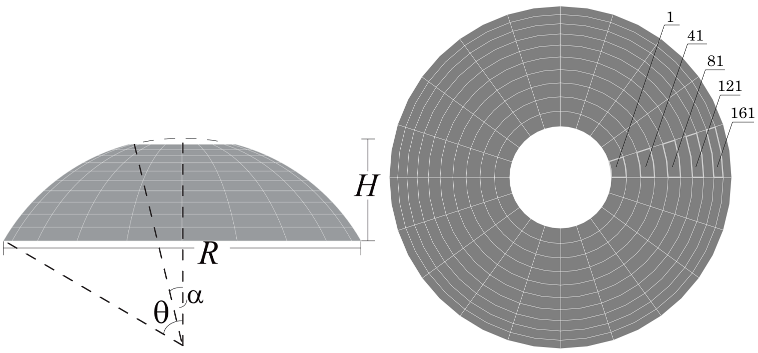

Fig. 1 A spherical shell model.

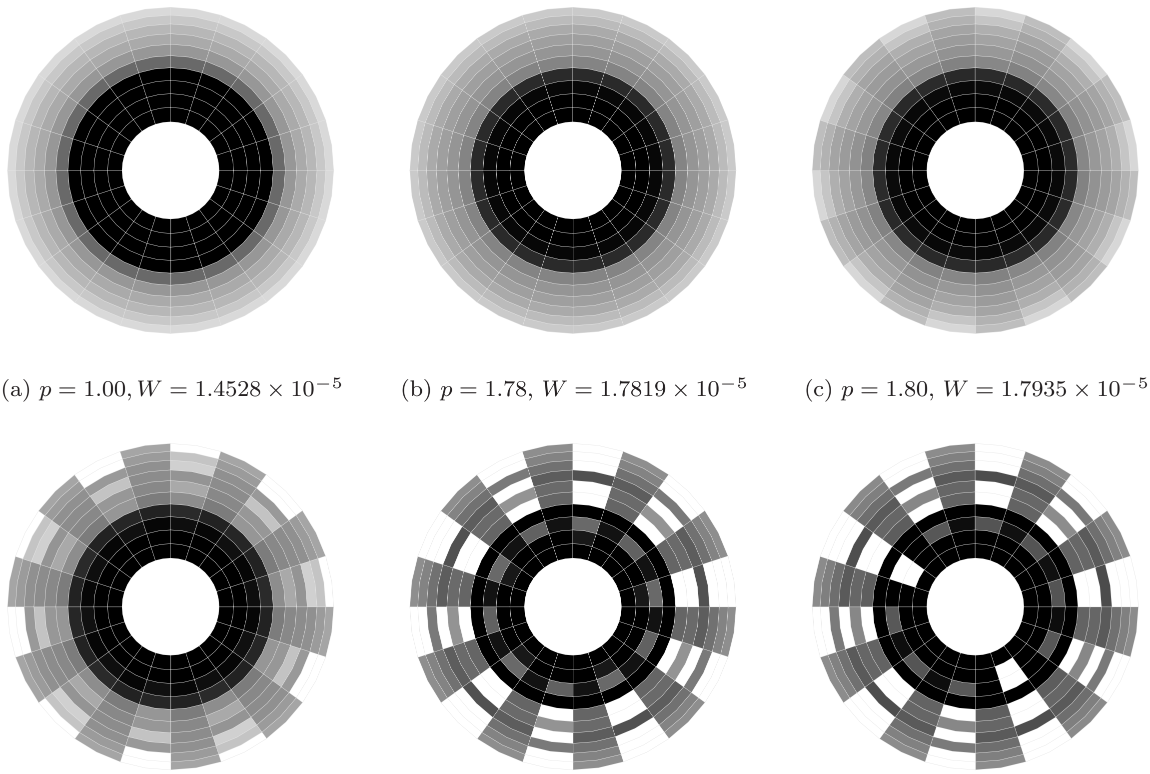

(a) $p = 1.00, W = 1.4528 \times 10^{-5}$ (b) $p = 1.78$, $W = 1.7819 \times 10^{-5}$ (c) $p = 1.80$, $W = 1.7935 \times 10^{-5}$

(d) $p = 1.82$, $W = 1.7947 \times 10^{-5}$ (e) $p = 2.94$, $W = 2.2391 \times 10^{-5}$ (f) $p = 2.96$, $W = 2.2148 \times 10^{-5}$

Fig. 2 Optimal solutions for various values of parameter p.

usually satisfied because d_i has moderately large value for the elements in $\mathcal{I}$.

Suppose there exists a singular point where the lowest eigenvalue of $\mathbf{B}^{22*}$ vanishes. The rate form (22) is converted to an incremental form as follows for the increments $\delta\mathbf{d}_0$ and $\delta\lambda$ of $\mathbf{d}_0$ and λ, respectively, corresponding to the increment δp of the parameter:

$$\begin{pmatrix} \mathbf{B}^{22*} & \mathbf{B}^{23} \\ \mathbf{B}^{23\top} & 0 \end{pmatrix} \begin{pmatrix} \delta\mathbf{d}_0 \\ \delta\lambda \end{pmatrix} = \delta p \begin{pmatrix} \mathbf{b}^{2*} \\ 0 \end{pmatrix} \tag{28}$$

As seen from (20c), the elements of vector $\mathbf{B}^{23}$ has nonzero values, and $\mathbf{B}^{23}$ has the same symmetry property as the solution with uniform density. Let $\mathbf{\Phi}$ denote the eigenvector corresponding to the zero eigenvalue of $\mathbf{B}^{22*}$; i.e., the kernel of the matrix $\mathbf{B}^{22*}$ is given as $c\mathbf{\Phi}$ with arbitrary coefficient c. If $\mathbf{\Phi}$ has a lower symmetry property than $\mathbf{B}^{23}$, then $\mathbf{\Phi}^\top\mathbf{B}^{23} = 0$ and $\mathbf{B}^{23}$ is included in the range of $\mathbf{B}^{22*}$. In this case, for the constant parameter value, i.e., $\delta p = 0$, there exists a solution $\delta\mathbf{d}_0 = \beta\mathbf{\Phi}$ and $\delta\lambda = 0$ with β being an arbitrary

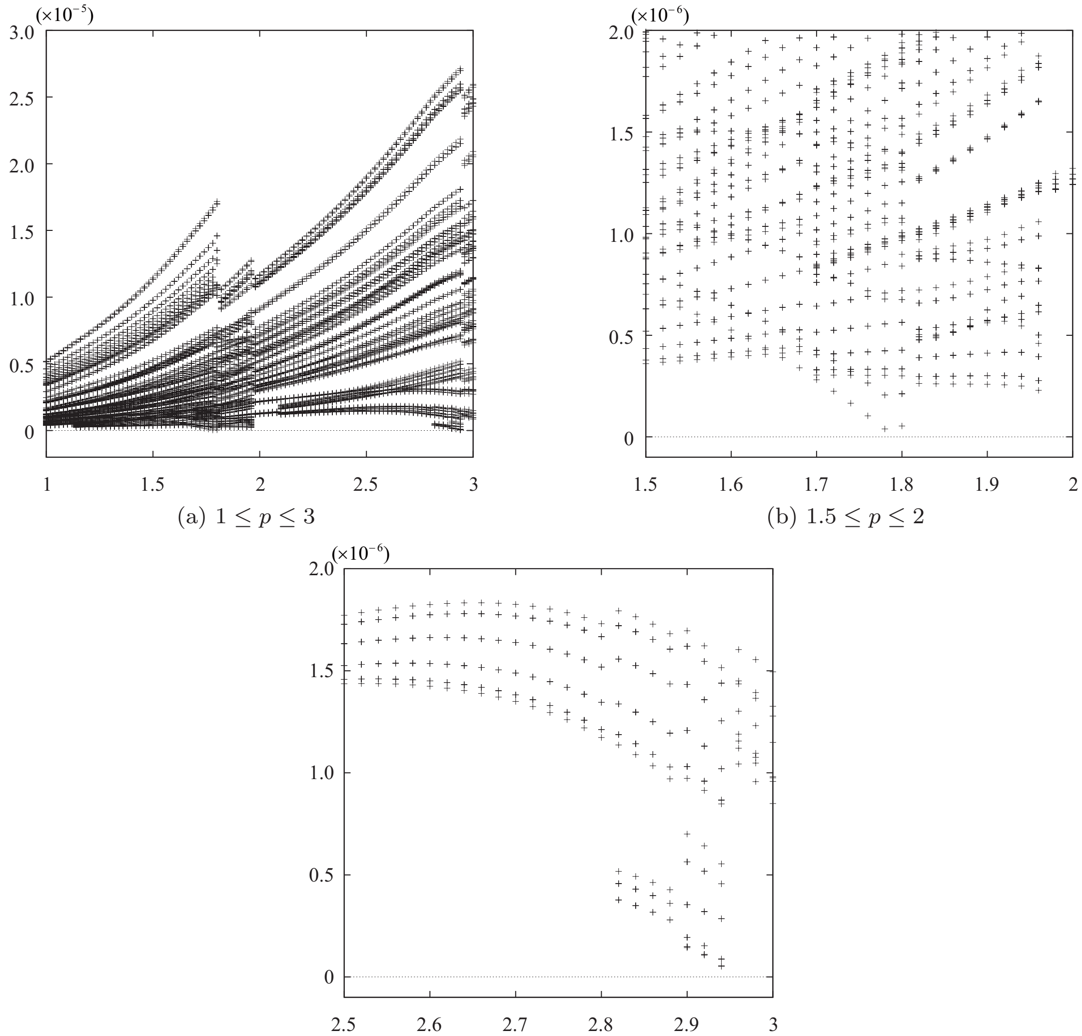

(a) $1 \leq p \leq 3$

(b) $1.5 \leq p \leq 2$

(c) $2.5 \leq p \leq 3$

Fig. 3 Eigenvalues of the matrix $\mathbf{B}^{22*}$.

nonzero value. It is easily observed from (20d), (20e), and (23) that $\mathbf{b}^{2*}$ has the same symmetry property as the current optimal solution. Therefore, if $\mathbf{\Phi}^\top \mathbf{b}^{2*} = 0$, i.e., if $\mathbf{b}^{2*}$ is included in the range of $\mathbf{B}^{22*}$, then there exists a particular solution that may have nonzero value of δp. Hence, bifurcation of solution occurs when $\mathbf{B}^{22*}$ becomes singular.

Jog and Haber (1996) derived the conditions of uniqueness and stability of the optimal solution based on incremental form of variational problem. They first used continuum formulation that is reduced to a finite element formulation. In the following, we summarize their results in a matrix-vector form.

The optimization problem is formulated as a max-min problem:

$$\text{find} \ \max_{\mathbf{d}} \min_{\mathbf{U}} \frac{1}{2}\mathbf{U}^\top \mathbf{K}\mathbf{U} - \mathbf{P}^\top \mathbf{U}$$
$$-\lambda \left(\sum_{i=1}^{m} d_i - \bar{V} \right) - \gamma \left(\sum_{i=1}^{m} d_i(1-d_i) \right) \tag{29a}$$
$$\text{subject to} \ \ 0 \leq d_j \leq 1, \quad (j = 1, \dots, m) \tag{29b}$$

where γ is the penalty parameter. From the stationary conditions of the Lagrangian of Problem (29), we obtain the equilibrium equation (6) and the optimality conditions (13) for the elements in $\mathcal{I}$, where $G_i(\mathbf{d})$ in (13) is to be replaced by

$$G_i(\mathbf{d}) = p d_i^{p-1} \mathbf{U}^\top \mathbf{K}_i \mathbf{U} + 2\lambda - 2\gamma(1 - 2d_i) \tag{30}$$

The incremental equations are derived in the following form for solving the equilibrium equations and optimal-

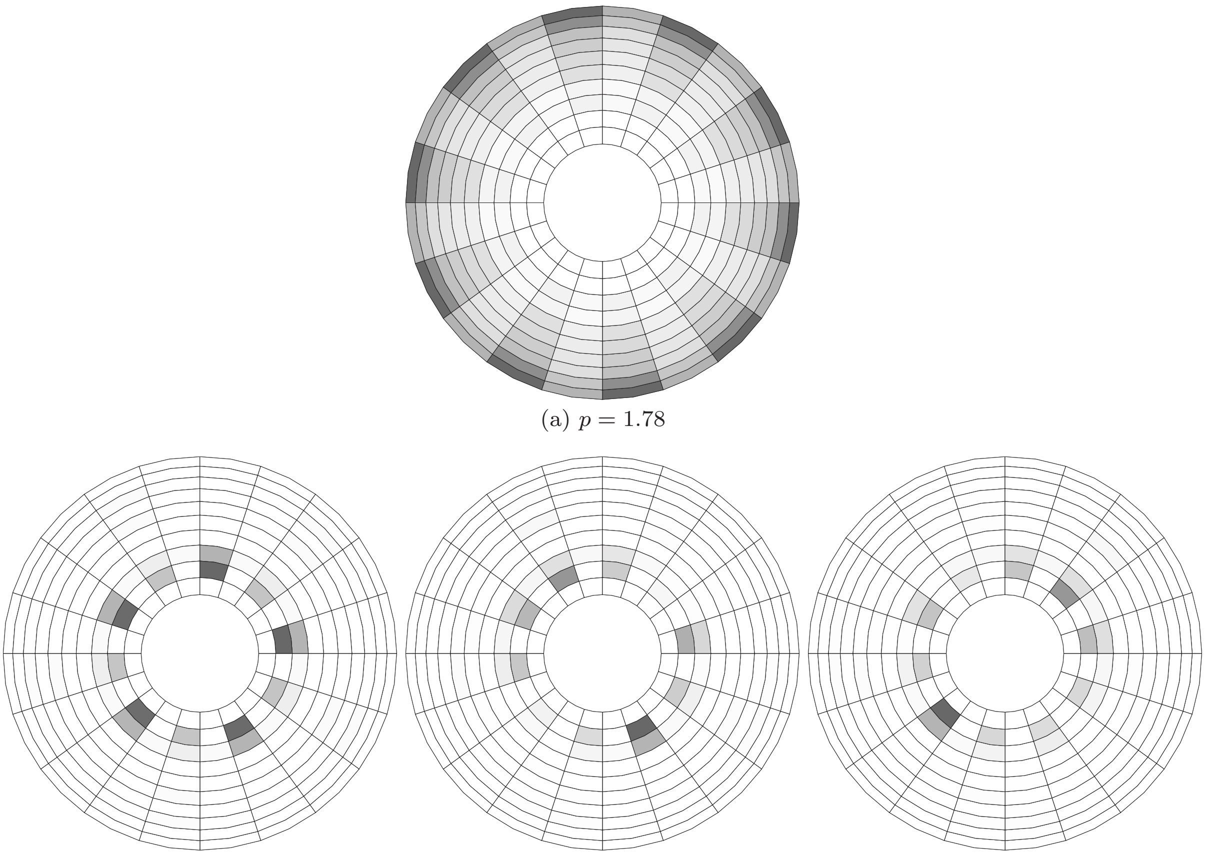

(a) $p = 1.78$

(b-1) $p = 2.94$ (b-2) $p = 2.94$ (b-3) $p = 2.94$

Fig. 4 Eigenvectors of $\mathbf{B}^{22*}$ for $p = 1.78$ and 2.94.

ity conditions using Newton iteration:

$$\begin{pmatrix} \mathbf{K} & \mathbf{B}^{12} \\ \mathbf{B}^{12\top} & \mathbf{B}^{22} \end{pmatrix} \begin{pmatrix} \delta\mathbf{U} \\ \delta\mathbf{d}_0 \end{pmatrix} = \begin{pmatrix} \mathbf{b}^1 \\ \mathbf{b}^2 \end{pmatrix} \tag{31}$$

with appropriate modification of matrices and vectors due to incorporation of the penalty term $\gamma d_i(1-d_i)$ and the differences in the signs of the strain energy in the objective function. Note that the increment of λ is not considered in (31), i.e., λ is fixed for some reason in the iterative process. Then, the conditions of uniqueness of the solution are: $\mathbf{K}$ is positive definite and $\mathbf{B}^{22}$ is negative definite.

6 Numerical examples

As a numerical example, uniqueness and symmetry of optimal solution is investigated for an axisymmetric shell. The symmetry of the solution is indicated using the standard notations of group theory (Kettle, 2007). If the solution does not change after application of reflection with respect to one of n different planes containing the axis of symmetry, and also with respect to rotation of one of n different angles around the axis of symmetry, then it has the dihedral symmetry D_n.

Consider a spherical shell as shown in Fig. 1 subjected to the vertical concentrated load P at each node on the top ring. The design domain is discretized to 10 and 20 elements in longitudinal and circumferential directions, respectively, i.e., the total number of elements is 400. The geometrical parameters are $R = 40.0$ m, $H = 11.5$ m, $\theta = \pi/3$, and $\alpha = \pi/12$. Young's modulus is 2.10×10^8 kN/m^2, Poisson's ratio is 0.3, and $P = 1.0$ kN. In the following, the units of length and force are m and kN, respectively, which are omitted for brevity. However, the objective function is multiplied by 10^9 to prevent numerical difficulty. The values in the figures are those without scaling. The small density parameter for ε for preventing numerical instability is 1.0×10^{-6}, the maximum thickness is $h_i = 0.5$ m, and the upper-bound volume $\bar{V}$ is 50% of the value of the solution with $d_i = 1$ for all elements. Optimization is carried out using SNOPT Ver. 7 (Gill *et al.*, 2002), where the sequential quadratic programming (SQP) is used. The default values are used for the parameters except the strict tolerance 10^{-12} for feasibility. The tolerance

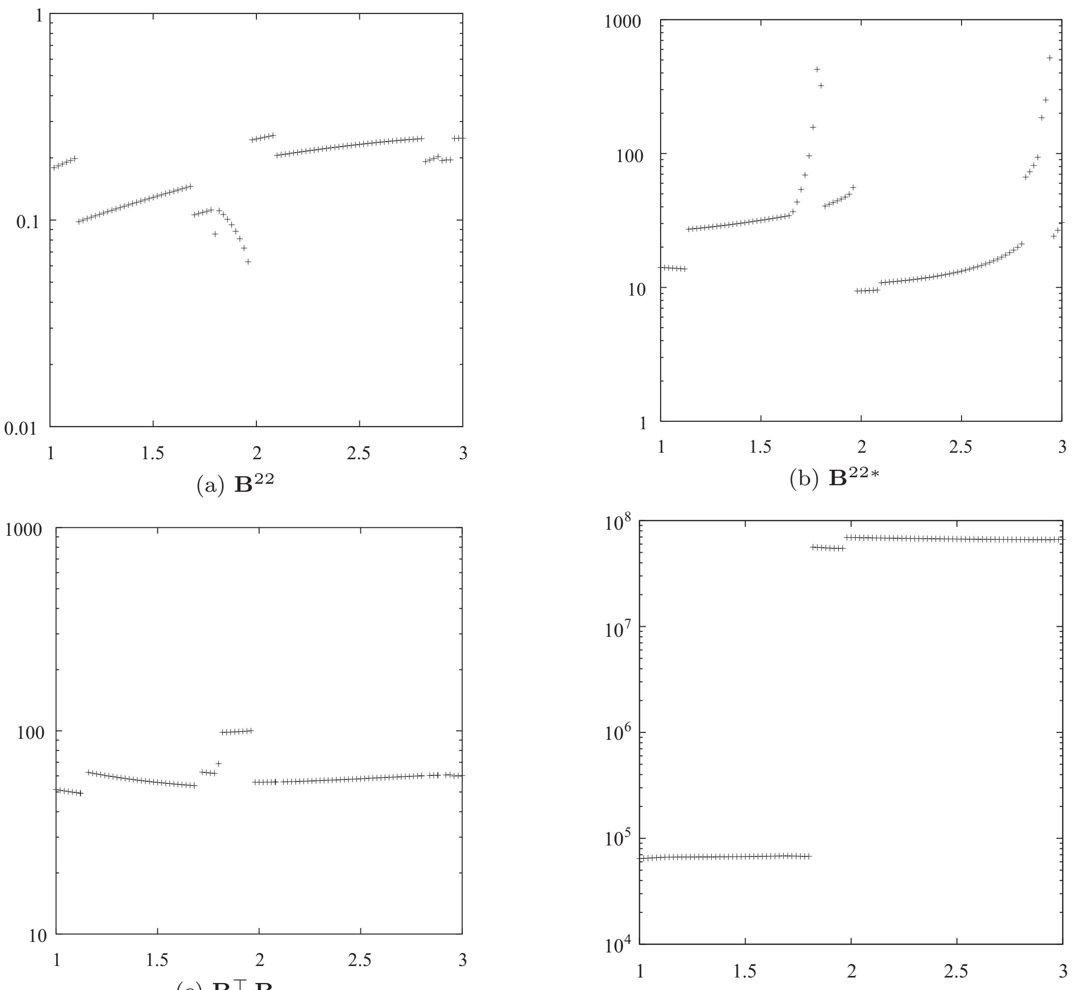

(a) $\mathbf{B}^{22}$ (b) $\mathbf{B}^{22*}$ (c) $\mathbf{B}_{12}^{\top}\mathbf{B}_{12}$ (d) $\mathbf{K}$

Fig. 5 Variations of condition numbers.

of optimality is also small enough so that optimization is carried out until no improvement is achieved.

The parametric sensitivity coefficients of optimal solutions are first verified. For $p = 1.0$, the optimal densities of the elements 1, 41, 81, 121, and 161 indicated in Fig. 1 are $d_1 = d_{41} = 1.0000$, $d_{81} = 0.58805$, $d_{121} = 0.33348$, and $d_{161} = 0.21647$. The sensitivity coefficients are obtained as $d'_1 = d'_{41} = 0$, $d'_{81} = -0.3232$, $d'_{121} = 0.05138$, and $d'_{161} = 0.06652$. The sensitivity coefficients obtained by the forward finite difference approach with $\Delta p = 0.01$ are $d'_1 = d'_{41} = 0$, $d'_{81} = -0.3226$, $d'_{121} = 0.05133$, and $d'_{161} = 0.06640$, which have good agreement with the analytical results.

Local optimal solutions are found for the parameters between $p = 1.0$ and 3.0 with the increment $\Delta p = 0.02$, by tracing a solution path assigning the solution of $p - \Delta p$ as the initial solution for the SQP algorithm. Fig. 2 shows the distributions of d_i of optimal solutions for various parameter values in gray scale. The values of the objective function W are also shown. The same axisymmetric solution is found from any initial solution for $p = 1.0$, because the objective function is convex and the volume constraint is linear with respect to $\mathbf{d}$. Optimization in the parameter range $1.00 \leq p \leq 1.78$ leads to axisymmetric solutions as shown in Fig. 2(a) and (b), which have D_{20}-symmetry.

For each parameter value, the eigenvalues of $\mathbf{B}^{22*}$ of the KKT point are plotted in Fig. 3. As seen in Fig. 3(b), the matrix $\mathbf{B}^{22*}$ becomes singular with a zero eigenvalue between $p = 1.78$ and 1.80. Accordingly, the symmetry of solution for $p = 1.80$ in Fig. 2(c) is reduced to D_{10}, and the difference between the two solutions for $p = 1.78$ and 1.80 is proportional to the eigenvector corresponding to the zero eigenvalue of the optimal solution for $p = 1.78$, which has D_{10}-symmetry as shown in Fig. 4(a).

The condition numbers of $\mathbf{B}^{22}$, $\mathbf{B}^{22*}$, $\mathbf{B}_{12}^{\top}\mathbf{B}_{12}$, and $\mathbf{K}$ are plotted in log-scale in Fig. 5. The norm of para-

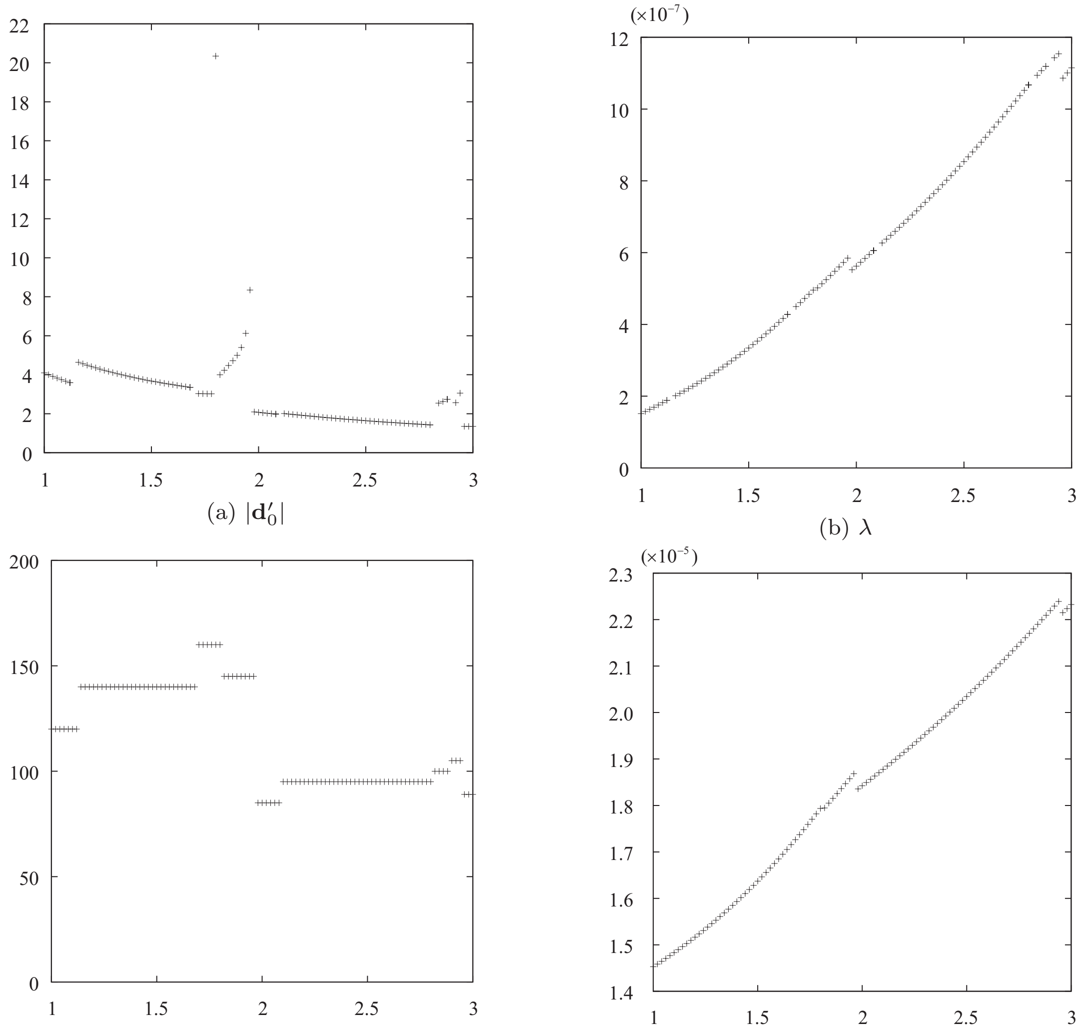

(a) $|\mathbf{d}'_0|$ (b) λ (c) s (d) W

Fig. 6 Variations of the norm of parametric sensitivity vector $|\mathbf{d}'_0|$, Lagrange multiplier λ, cardinality s of $\mathcal{I}$, and objective function W.

metric sensitivity vector, Lagrange multiplier, cardinality s of $\mathcal{I}$, and objective function are plotted in Fig. 6. As is seen, the condition number of $\mathbf{B}^{22*}$ and the norm $|\mathbf{d}'_0|$ of parametric sensitivity vector drastically increase around $p = 1.78$ at which $\mathbf{B}^{22*}$ has very small positive eigenvalue. It is also seen from Fig. 5 that the $n \times s$ matrix $\mathbf{B}^{12}$ has full column rank s ($< n$). The condition number of $\mathbf{K}$ jumps to a very large value at the singular point of $\mathbf{B}^{22*}$; however, $\mathbf{B}^{22*}$ has moderately small condition number in the range $p \geq 1.80$, although the condition number of $\mathbf{K}$ is very large. For $p = 2.0$, the condition number of $\mathbf{K}$ is 6.913×10^7, which is very large; i.e., $\mathbf{U}$ is nearly nonunique. By contrast, the condition numbers of $\mathbf{B}_{22}$ and $\mathbf{B}^*_{22}$ are 0.2469 and 9.413, respectively, which are sufficiently small. Therefore, instability of the structure, or nonuniqueness of the displacement vector $\mathbf{U}$ is not related to the bifurcation of the optimal solution.

More symmetry-breaking singular points can be found by further increasing the parameter p. The solution for $p = 1.82$ has D_5-symmetry as shown in Fig. 2(d), and the solutions in the parameter range $1.82 \leq p \leq 2.94$ have the same symmetry property, because $\mathbf{B}^{22*}$ remains to be positive definite. The lowest eigenvalue of $\mathbf{B}^{22*}$ becomes zero between the parameter range $2.94 \leq p \leq 2.96$, and the symmetry of the solution reduces from D_5 to D_2 as shown in Fig. 2(d) and (e). For $p = 2.94$, the lowest eigenvalues of $\mathbf{B}^{22*}$ are threefold, for which the eigenvectors are shown in Fig. 4, where (b-1) and (b-3) have D_5 and D_1-symmetry, respectively, while (b-2) does not have any symmetry property.

There also exist other points at which the lowest eigenvalue of the matrix $\mathbf{B}^{22*}$ and the condition num-

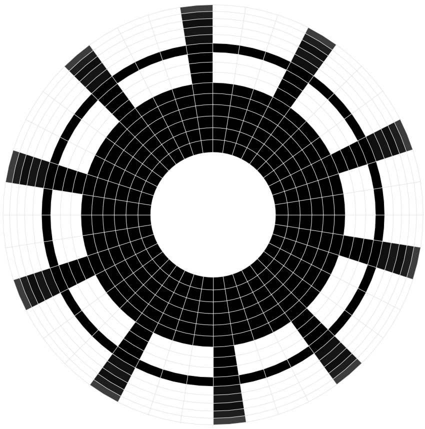

(a)

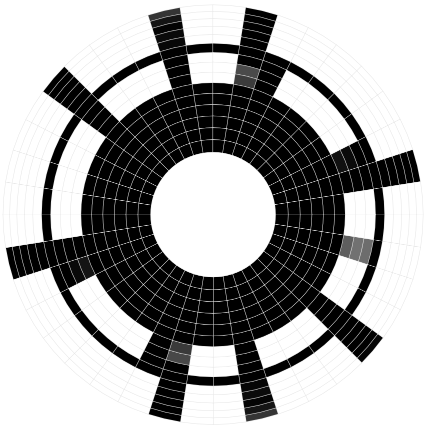

(b)

Fig. 7 Optimal topology of 15×40 model with $p = 3$; (a) continuation approach, (b) direct optimization.

bers of the matrix $\mathbf{B}^{22}$ and $\mathbf{B}^{22*}$ jump discontinuously due to the variation of the size s of these matrices.

Since the shape is fixed and only the topology is varied, the mechanism of resisting external loads distributed around the top ring did not change as an result of increasing the penalization parameter.

Finally, optimal topologies are found for a finer mesh with 15 and 40 elements in longitudinal and circumferential directions, respectively, i.e., the total number of elements is 600. Starting with the uniform initial design $d_i = 0.5$ for all elements with $p = 1.0$, the parameter p is increased to 3.0 with the increment 0.01. The optimal topology obtained in this continuation approach is shown in Fig. 7(a). As is seen, a topology with D_{10}-symmetry has been obtained; however, some

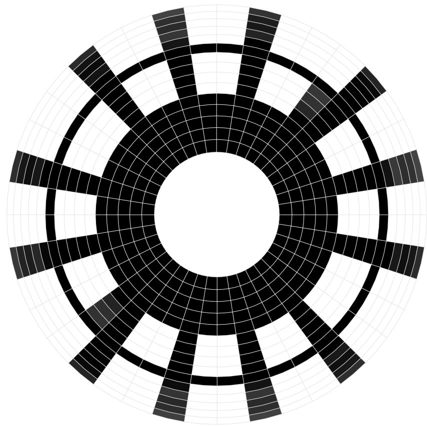

Fig. 8 Optimal topology of 15×40 model with $p = 4$; direct optimization.

gray elements exist near the boundary. In contrast, if we optimize directly for $p = 3.0$ from the uniform initial solution, then the topology as shown in Fig. 7(b) is obtained. As is seen, no clear symmetry is observed.

The optimal topology for $p = 4.0$ using continuation approach is shown in Fig. 8(a). An almost clear 0–1 solution has been found with $d_i = 1.0$ for 341 elements, $0.966 \leq d_i \leq 0.968$ for 10 elements, and $d_i = 0.0$ for 249 elements. The number of elements with $d_i \simeq 1.0$ is not equal to the half of the total number elements, because the elements around the boundary have larger area than those around the center. If we optimize directly for $p = 4.0$ from the uniform initial solution, then the topology is obtained as shown in Fig. 8(b), which has no clear symmetry.

7 Conclusions

A simple formulation has been presented for investigating the path of the first-order optimal solution of an axisymmetric shell that minimizes the compliance under specified load and the total structural volume. The conditions of nonuniqueness of the solution are derived based on a bifurcation of the solution path with respect to the penalization parameter of the SIMP approach. The formulation for numerical continuation with respect to the penalization parameter is rigorously derived by differentiating the KKT conditions, stiffness (equilibrium) equations, and volume constraint.

The main results are summarized as follows:

1. The symmetry reduction process of the KKT point can be defined as an bifurcation of solution path

with respect to the penalization parameter of SIMP approach.
2. Convergence of optimization algorithm and uniqueness of solution path are defined by the same condition of the singularity of a matrix similarly to geometrically nonlinear analysis of structures.
3. Nonuniqueness of displacement does not have any effect on nonuniqueness of the KKT point.
4. It has been shown quantitatively that symmetry of KKT point reduces through bifurcation to the critical eigenvector of the Jacobian of the governing equations in the continuation process of KKT point using SIMP approach.
5. A procedure has been developed for detecting bifurcation of the solution and the direction of reduction of symmetry using eigenvalue analysis of the Jacobian of the governing equations. A procedure has also been developed for condensing Jacobian to remove the derivatives of displacements and separate the nonuniqueness properties of displacements and design variables.

Thus, a unified approach has been presented for investigation of uniqueness and bifurcation (symmetry-breaking process) of KKT point. A local optimal solution with appropriate symmetry can be found through investigation of symmetry using continuation approach. Note that the symmetry properties without filter can be used for appropriately setting the parameters for filters and other regularization.

The numerical example of an axisymmetric shell shows that a solution path of an axisymmetric shell has a bifurcation point where the Jacobian of the governing equations is singular. The KKT point is nonunique at the bifurcation point, and a symmetry-breaking bifurcation path exists in the direction of the eigenvector corresponding to the zero eigenvalue analyses of the Jacobian. This way, the symmetry-reduction process of the KKT point is characterized as a bifurcation process of a solution path with respect to the penalization parameter. Although the solution with intermediate density has no practical meaning, it is important to investigate the symmetry breaking process of the KKT point on the basis of bifurcation of a solution path.

The condition numbers of the matrix for computing the sensitivity coefficients of the KKT points, and the corresponding sub-matrices, have been computed to show that nearly singular stiffness matrix does not lead to nonuniqueness of the KKT point.

Note that the proposed method is effective for any problem with symmetry including a circular disc subjected to a twisting force at the center circle, which is often used as an example of Michell structure. We used a shell structure, because it has high symmetry. Furthermore, the method proposed in this paper can also be used for the case where a filter is used, and it can be applied to a large-scale problem without any difficulty, because the eigenvalue analysis should be carried out for the matrix of the size equal to the variables that have intermediate values.

References

Allaire, G., Jouve, F., and Toader, A. M. (2002). A level set method for shape optimization. *Comptes Rendus de l' Acad. des Sci.*, **334**, 1125–1130.

Allaire, G., Jouve, F., and Toader, A. M. (2004). Structural optimization using sensitivity analysis and a level-set method. *J. Comp. Phys.*, **104**, 363–393.

Allgower, E. L. and Georg, K. (1993). Continuation and path following. *Acta Numerica*, **2**, 1–64.

Belblidia, F. and Bulman, S. (2002). A hybrid topology optimization algorithm for static and vibrating shell structures. *Int. J. Num. Meth. Engng.*, **24**, 835–852.

Bendsøe, M. P. (1989). Optimal shape design as a material distribution problem. *Structural Optimization*, **1**, 193–202.

Bendsøe, M. P. and Kikuchi, N. (1988). Generating optimal topologies in structural design using a homogenization method. *Comp. Meth. Appl. Mech. Engng.*, **71**, 197–224.

Bendsøe, M. P. and Sigmund, O. (2003). *Topology Optimization: Theory, Methods and Applications*. Springer, Berlin.

Bruns, T. E. (2005). A reevaluation of the SIMP method with filtering and an alternative formulation for solid–void topology optimization. *Struct. Multidisc. Optim.*, **30**, 428–436.

Bruns, T. E. (2007). Topology optimization by penalty (TOP) method. *Comp. Meth. Appl. Mech. Engng.*, **196**, 4430–4443.

Choi, K. K. and Kim, N.-H. (2004). *Structural sensitivity Analysis and Optimization 1, Linear Systems*. Springer, New York.

Fiacco, A. V. (1983). *Introduction to Sensitivity and Stability Analysis in Nonlinear Programming*. Academic press.

Gal, T. (1979). *Postoptimal Analyses, Parametric Programming, and Related Topics*. Mc-Graw Hill.

Gill, P. E., Murray, W., and Saunders, M. A. (2002). SNOPT: An SQP algorithm for large-scale constrained optimization. *SIAM Journal on Optimization*, **12**, 979–1006.

Golubitsky, M. and Schaegger, D. (1979). A theory for imperfect bifurcation via singularity theory. *Comm. Pure and Appl. Math.*, **32**, 21–98.

Ikeda, K. and Murota, K. (2002). *Imperfect Bifurcation Phenomena in Structures and Materials – An Engineering Use of Group-theoretic Bifurcation Theory.* Appl. Math. Sci. Ser. 149. Springer, New York, NY.

Jog, C. S. and Haber, R. B. (1996). Stability of finite element models for distributed-parameter optimization and topology design. *Comp. Meth. Appl. Mech. Engng.*, **130**, 203–226.

Kanno, Y., Ohsaki, M., Murota, K., and Katoh, N. (2001). Group symmetry in interior-point methods for semi-definite program. *Optimization and Engineering*, **2**, 293–320.

Kettle, S. F. A. (2007). *Symmetry and Structure: Readable Group Theory for Chemists.* John Wiley & Sons, Chichester, UK.

Kočvara, M. and Outrata, J. V. (2006). Effective reformulation of the truss topology design problem. *Optimization and Eng.*, **7**, 201–219.

Martínez, J. M. (2005). A note on the theoretical convergence properties of the SIMP method. *Struct. Multidisc. Optim.*, **29**, 319–323.

Maute, K. and Ramm, E. (1997). Adaptive topology optimization of shell structures. *AIAA J.*, **35**, 1767–1773.

Mittelmann, H. D. and Roose, D., editors (1990). *Continuation Techniques and Bifurcation Problems.* Birkhäuser Verlag, Basel, Germany.

Moses, E., Fuchs, M. B., and Ryvkin, M. (2003). Topology design of modular structures under arbitrary loading. *Struct. Multidisc. Optim.*, **24**, 407–417.

Nakamura, T. and Ohsaki, M. (1988). Sequential optimal truss generator for frequency ranges. *Comp. Meth. Appl. Mech. Engng.*, **67**(2), 189–209.

Ohsaki, M. (2006). Local and global searches of approximate optimal designs of regular frames. *Int. J. Num. Meth. Engng.*, **67**, 132–147.

Ohsaki, M. and Ikeda, K. (2007). *Stability and Optimization of Structures – Generalized Sensitivity Analysis.* Mechanical Engineering Series. Springer, New York.

Ohsaki, M. and Nakamura, T. (1996). Minimum constraint perturbation method for topology optimization of systems. *Eng. Opt.*, **26**, 171–186.

Petersson, J. (1999a). A finite element analysis of optimal variable thickness sheets. *SIAM J. Mumer. Anal.*, **36**(6), 1759–1778.

Petersson, J. (1999b). Some convergence results of perimeter-controlled topology optimization. *Comp. Meth. Appl. Mech. Engng.*, **171**, 121–140.

Petersson, J. and Sigmund, O. (1998). Slope constrained topology optimization. *Int. J. Num. Meth. Engng.*, **41**, 1417–1434.

Rietz, A. (2001). Sufficiency of a finite exponent in SIMP (power law) methods. *Struct. Multidisc. Optim.*, **21**, 159–163.

Rietz, A. (2007). Modified conditions for minimum of compliance. *Comp. Meth. Appl. Mech. Engng.*, **196**, 4413–4418.

Rozvany, G. I. N. (2009). A critical review of established methods of structural topology optimization. *Struct. Multidisc. Optim.*, **37**, 217–237.

Rozvany, G. I. N. (2011). On symmetry and nonuniqueness in exact topology optimization. *Struct. Multidisc. Optim.* published online, DOI: 10.1007/s00158-010?0564-0.

Rozvany, G. I. N., Zhou, M., and Birker, T. (1992). Generalized shape optimization without homogenization. *Struct. Optim.*, **4**, 250–252.

Rozvany, G. I. N., Zhou, M., and Sigmund, O. (1994). Topology optimization. In H. Adeli, editor, *Advances in Design Optimization*, chapter 10. Chapman and Hall, London.

Sethian, J. A. and Wiegmann, A. (2000). Structural boundary design via level-set and immersed interface methods. *J. Comput. Phys.*, **163**(2), 489–528.

Stolpe, M. (2010). On some fundamental properties of structural topology optimization problems. *Struct. Multidisc. Optim.*, **41**, 661–670.

Stolpe, M. and Svanberg, K. (2001). On the trajectories of the epsilon-relaxation approach for stress-constrained truss topology optimization. *Struct. Multidisc. Optim.*, **21**, 140–151.

Suzuki, K. and Kikuchi, N. (1991). A homogenization method for shape and topology optimization. *Comp. Meth. Appl. Mech. Engng.*, **93**, 291–318.

Wang, M. Y., Wang, X. M., and Guo, D. M. (2003). A level set method for structural topology optimization. *Comp. Meth. Appl. Mech. Engng.*, **192**, 227–246.

Watson, L. T. and Haftka, R. T. (1989). Modern homotopy methods in optimization. *Comp. Meth. Appl. Mech. Engng.*, **74**(3), 289–305.

Yamada, T., Nishiwaki, S., Izui, K., Yoshimura, M., and Takezawa, A. (2009). A new level set based topology optimization method using a fictitious interface energy model based on phase field method concepts. In *Proc. 8th World Congress of Structural and Multidisciplinary Optimization (WCSMO8)*, number Paper No. 1136, Lisbon.

Yamasaki, S., Nomura, T., Kawamoto, A., Sato, K., Izui, K., and Nishiwaki, S. (2010). A level set based topology optimization method using the discretized signed distance function as the design variables. *Struct. Multidisc. Optim.*, **41**, 685–698.